Study of the Effect of Geomembranes on the Interaction between the Soil and Underground Structures

Ahmed S. Rashed[1], Tamer M. Sorour[2], Ahmed N. Elsayed[1]

[1] Geotechnical Engineering and Foundations, Civil Engineering Department, Higher Institute of Engineering, at El-Shorouk City, Cairo, Egypt
[2] Structural Engineering Department, Faculty of Engineering, Ain Shams University, Cairo, Egypt
Emails: ELrashed6000@yahoo.com, tamer.sorour@eng.asu.edu.eg, a.nabel@sha.edu.eg

Abstract-Geomembranes are widely used as insulation materials in different civil engineering applications. Failure due to the slippage between geomembranes and the interfacing soils was detected at some cases. This research investigated the factors controlling the developed interface stresses strength between the soil and geomembranes. In order to quantify the effect of different commonly used isolation membranes on the behavior and stability of buried concrete structures, laboratory studies by using modified direct shear apparatus is performed and integrated and the reduction in the shear resistance between the soil and different types of isolation geomembranes is determined. Graded sand with well-rounded particles was used in the experimental program. Shear tests were applied under a normal stress range of about 25-100 kPa. The effect of the geomembranes on the peak and residual interface shear strengths is highlighted. Test's results indicate development of peak interface shear resistance at a small strain and constant residual interface shear resistance at large strain. It was found that the developed peak and residual interface friction angles between the sand and the geomembranes interfaces ranged from 59 % to 82 % of the corresponding angles between sand and un-protected concrete.

Keywords- Geomembranes; Interface shear; sand; dry condition.

I. INTRODUCTION

Insulation membranes are commonly used for protecting underground structures from the effect of subsurface aggressive environments containing high concentrations of chlorides and sulphates. Interaction between the surface of buried concrete elements as retaining walls, foundations and the surrounding soils depends mainly on the shear resistance that is adversely affected by the presence of such membranes.

The problem we are dealing with in this paper is the effect of different commonly used insulation membranes on the behavior and stability of buried concrete structures. The contribution of this paper is to quantify the reduction in the shear resistance of soils in contact with buried concrete elements protected by using various types of insulation geomembranes.

This paper is organized as follows: section II gives the literature review, section III gives the experimental program, section IV gives the experimental program, section V gives the analysis and discussion, and section VI gives the experimental program.

II. LITERATURE REVIEW

The studies of the soil-geomembrane interface shear strength started in the early of 1980's. After a failure of a large landfill in California in USA [1], many of researchers have conducted extensive studies to find the cause of landfill collapse. This collapse occurred when a large mass of waste materials slide along the interface with the geomembranes layer [2, 3]. The common test used to determine the interface shear strength between soils and other materials is the standard direct shear test [4]. The direct shear box is one of the most reliable techniques for the interface shear strength testing [5]. In 1992, the geomembranes Research Institute at Drexel University in USA adopted the first standard technique to evaluate the interface shear strength parameters [6].

A series of experimental tests were performed to study the interfaces shear strength between the sand and the different types of geomembranes [2], it was conducted using a modified direct shear machine. The used normal stresses levels in this study were ranged from 13.8 kPa to 103.5 kPa. The test results found that the interface friction angles between the sand and the smooth geomembrane around 18°. Another experimental work was performed to study the soil and the geomembranes interface friction angle [7], a series of interfaces were tested by using a ring shear apparatus.

The test results revealed that the peak resistance develops at a small strain and the residual interface friction angle was constant at a large strain. The test's results also showed that the increase in the angularity of the sand grains causes an increase in the interface friction angle. The peak and residual interface friction angles between the Ottawa sand and geomembranes were found to be in the range between 17.60° and 15.0° respectively compared with the residual interface friction angle of 30.50° for the Ottawa sand.

Another experimental work was conducted [8] to predict the interface friction of the smooth geomembranes and sand soil in order to prevent the slippage failures between the geomembranes materials and the interfacing soils. Laboratory tests were performed using a ring shear strength apparatus to simulate the interface shear strength of various types of geomembranes and sand. The interface shear strength is governed by the imposed stress level and the stiffness and texture of the geomembranes. It was found that the residual interface friction angles (δr), for all of the geomembranes interfaces vary from 10.50° to 28.10°.

On the other hand, experimental work was conducted in [9] to study soil interface interaction. Several techniques have been developed to examine the interface behavior and to find the interface shear strength parameters. Moreover, experimental work was conducted in [10] to predict the effect of geomembranes surface roughness on interface friction angle. The tests showed that increasing the geomembrane asperity height and surface roughness caused an increase in the peak interface friction angle values.

In addition, experimental work was conducted using direct shear box [11] to study surcharge stress influence on smooth geomembranes – soil interface shear behavior. Normal stress has a large influence on the strength of coarse-grained interface. At stress levels below about 20 kPa for Ottawa sand, the friction coefficient decreases with increasing normal stress. This behaviour has practical implications for engineering applications at low stress levels, such as landfill covers, pond liners or upstream dam membrane liners. The friction coefficient is a minimum at the transition from sliding to plowing. For stress levels high, the friction coefficient increases with increasing normal stress. Another experimental work was conducted using three different sizes of shear box (60 × 60 mm2, 100 × 100 mm2 and 300 × 300 mm2) [12] to study effect of specimen size on direct shear test. Results indicate increasing the size of shear box decrease both of the peak shear strength and the peak friction angle and the residual shear strength remains constant.

Experimental work was also conducted by [13] to study the effect of the size of the shear box on the deduced Shear Strength Parameters. The results show that a slight increase in the values of the angle of internal friction as the size of the shear box decrease. Maximum variation in the angle of internal friction and the cohesion results was recorded with only 1.9° and 2.4 kPa, respectively.

III. EXPERIMENTAL PROGRAM

The purpose of this research is to investigate the reduction in the shear resistance between the soil and different types of insulation geomembranes, experimentally using an assortment of modified direct shear tests, both of peak and residual interface friction angles are determined. The peak and residual interface friction angles between the soil and the geomembranes are a major factor in the design and analysis of geotechnical engineering projects where geomembranes materials are used such as retaining walls, pond liners, landfill covers or upstream dam membranes liners. The interface friction angle should be calculated accurately to prevent failures of structures.

A. Experimental Tools

The following section describes the tools used for this study.

- A tank, large enough to accommodate a concrete footing model.
- The concrete footing models for different types of insulation geomembranes are of reasonable sizes, considering the tank size.
- A loading system that provides a displacement control mode of loading.
- A suitable measurement technique for recording the test results to perform the shear strength-horizontal displacement curves.

I. Soil Container

The soil container (tank) is made of steel sheets. The inner dimensions were 1000 x 1000 mm2 with 600 mm height. The sides of the container are stiffened by additional steel sheets to prevent buckling of the sides during the soil compaction or testing procedure.

II. Loading System

The loading system consisted of three steel frames of 1000 mm span and spaced at 1000 mm. The three frames were connected together with a horizontal steel beam from the top in the two directions, where the mechanical screw jack is fixed in the middle of the beam of the third steel frames. Four steel angles at the bottom of the container are connected to the frame to increase the rigidity of the whole loading system. The load is transmitted from the mechanical screw jack to the footing sample through a proving ring and a horizontal loading bar, as indicated in Figure (1). The horizontal loading bar consists of a steel cylindrical shaft, which is fabricated to facilitate the changing of loading level, whether the footing sample is rested on the soil.

III. Load Recording

A proving ring is used, to specify the load transmitted to the model. The proving ring has a capacity restriction of 500 kg. The left side of the proving ring is connected to the mechanical screw jack, while its right side is connected to the loading bar, as illustrated in Figure (1). The proving ring is connected with dial gauge with an accuracy of 0.002 mm.

IV. Shear Displacement Rate

The rate doesn't affect the interface angle of friction significantly. Several studies have revealed that the peak and the residual friction angles of the soil-geomembranes interface don't change significantly due to changing the shear displacement rate [14], [15] and [16]. The loading rate of this model is 0.12 mm/min.

V. Displacement Recording

One horizontal dial gauge located at the middle side of the footing model is used to record the horizontal displacement of the footing model during loading, as shown in Figures (2) and (3). The compression of the horizontal loading bar is neglected due its high rigidity.

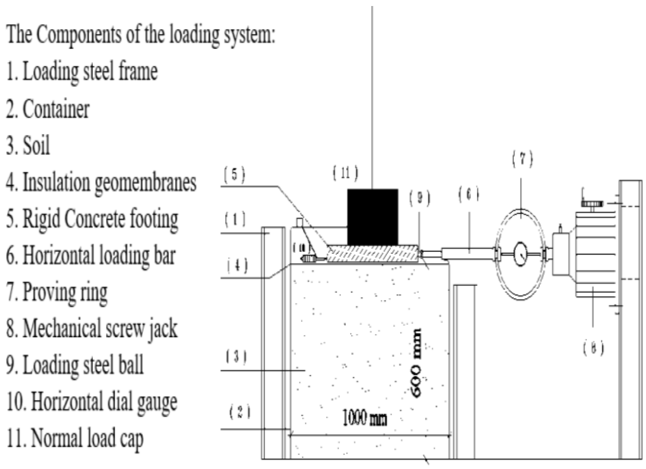

Figure 1. Schematic diagram for the model of modified direct shear test apparatus.

Figure 2. Test model component.

Figure 3. Test Setup.

B. Concrete Samples

Concrete specimens were prepared using ASTM C-109 standard testing method. The mortar composition is consisted of one part cement to 2 parts of graded sand to 3 parts of fine gravel with a water and cement ratio of 0.50. The samples were performed in cubes with dimensions (71 x 71 x 71 mm3) and allowed to curing with water for seven days and leaving sample for not less than 28 days after casting. After curing the samples, the surface of each specimen was cleaned with a fresh water, and it's allowed to dry for one day then installation the geomembranes samples as applying in Figure (4). The specimen's dimensions required maximum load of 50 kg to achieve normal stress 100 KPA during the test, which is similar to direct shear test according to ASTM D3080. Sample cap consists of square steel cap with upper dimensions (250 mm x 250 mm) and lower cavity with the same dimension of the concrete samples (71 mm x 71 mm) and it is equipped with an axial steel bar on its center to assure the right positioning of the loads on the concrete sample to avoid any eccentricity as illustrated in Figure (5).

Figure 4. Sample with the Geomembranes.

Figure 5. Sample with the Geomembranes.

C. Sand

The used soil was medium to coarse sand, the Unified Soil System classifies it as poorly graded sand. Figure 6 describes the grain size distribution curve for it. Direct shear test was used to determine shear strength parameters of the sand. Figure 7 presents the results of the tests. The angle of internal friction of the cohesion less sand (φ) was 34º, at Dr = 70%. The Properties of sand soil are listed in Table 1.

D. Geomembranes

Two types of MB geomembranes sheets are available:

- SBS polymer-modified bitumen geomembranes are installed in hot mopping of asphalt or cold adhesive. Some of it are modified to be self-adhering.
- APP polymer-modified bitumen geomembranes typically are heat-welded or torch-applied.

The type and roughness of geomembranes plays a significant role in determining the soil-geomembranes interface friction angle. Fifteen different kinds of APP Modified Bitumen geomembranes and SBS Modified Bitumen geomembranes are used in this study as shown in Figure (8), which are commonly used in Egypt, and which were manufactured by different Companies. The thickness of understudy geomembranes samples are between (3 mm to 6 mm). Table 2 shows the physical properties of these geomembranes materials, which were provided by the manufacturer.

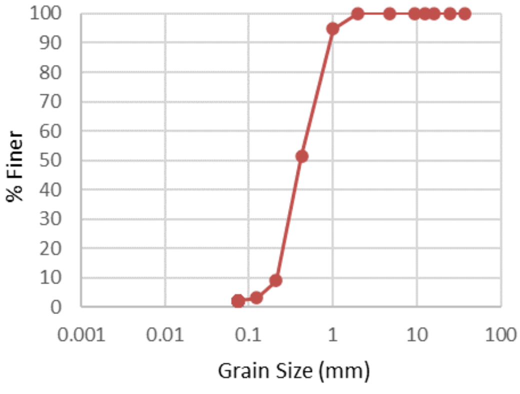

Figure 6. Sample with the Geomembranes.

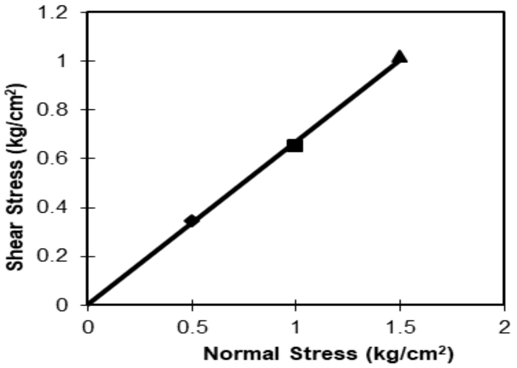

Figure 7. Direct shear test results of the sand soil.

Table 1. Properties of sand soil.

Description/property	Value
D10	0.22 (mm)
D30	0.30 (mm)
D60	0.50 (mm)
Coefficient of Uniformity (Cu)	2.332
Coefficient of curvature (Cc)	0.825
Maximum dry density	18.88 (kN/m^3)
Minimum dry density	14.43 (kN/m^3)
Angle of friction (φ)	34°
Specific gravity (Gs)	2.65
Relative density (Dr)	70%

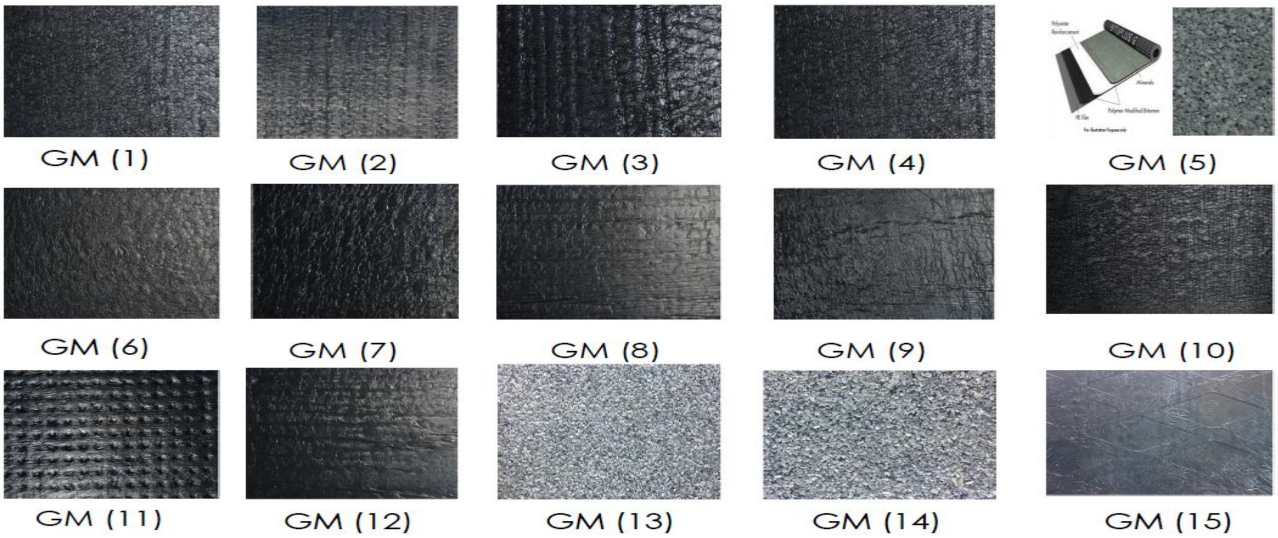

Figure 8. Geomembranes Samples.

Table 2. Properties of insulation geomembranes used in the tests.

Geomembrane Sample	Property								
	Thickness (mm)	Weight (kg/m2)	Roll Dimension		Tensile Strength		Elongation At Break		surface
			Width (m)`	Length (m)	Long. (N/5cm)	Tran. (N/5cm)	Long. (%)	Tran. (%)	
GM (1)	3	4	1	10	1050	750	45	45	smooth
	ASTM D5147	EN1849-1	EN1848-1		ASTM D5147		ASTM D5147		
GM (2)	3	4.3	1	10	750	600	≥ 40	≥ 42	smooth
	EN1849-1	EN1849-1	EN1848-1		EN12311-1		EN 12311-1		
GM (3)	3	4.2	1	10	850	700	15	15	smooth
	ASTM D5147	EN1849-1	EN1848-1		ASTM D5147		ASTM D5147		
GM (4)	3	–	1	10	850	600	40	45	smooth
	EN1849-1		EN1848-1		EN12311-1		EN12311-1		
GM (5)	3	3.7	1	10	400	300	25	35	slated
	EN1849-1	EN1849-1	EN1848-1		EN12311-1		EN12311-1		
GM (6)	4	–	1	10	750	550	35	40	smooth
	EN1849-1		EN1848-1		EN12311-1		EN12311-1		
GM (7)	4	4.5	1	10	700	500	40	45	smooth
	EN1849-1	EN1849-1	EN1848-1		EN12311-1		EN12311-1		
GM (8)	4	–	1	10	700	500	45	45	smooth
	ASTM D5147		UNI 8202		ASTM D5147		ASTM D5147		
GM (9)	4	–	1	10	850	650	40	45	smooth
	ASTM D5147		EN1848-1		ASTM D5147		ASTM D5146		
GM (10)	4	–	1	10	840	630	45	45	smooth
	UEAtc		EN1848-1		UEAtc		ASTM D146		
GM (11)	4	4.5	1	10	750	650	≥ 40	≥ 42	smooth

	EN1849-1	EN1849-1	EN1848-1		EN12311-1		EN12311-1		
GM (12)	4	–	1	10	800	550	30	35	smooth
	EN1849-1		EN1848-1		EN12311-1		EN12311-1		
GM (13)	4	5.2	–		950	850	50	50	slated
	ASTM D5147	UEAtc			ASTM D5147		ASTM D146		
GM (14)	4	–	1	10	840	630	45	45	slated
	UEAtc		EN1848-1		ASTM D146		ASTM D146		
GM (15)	6	6.7	1	10	–		–		smooth
	EN1849-1	EN1849-1	EN1848-1						

Figure 9. Compacting the Soil.

Figure 10. Fixing Ring and the Loading Bar.

Figure 11. The Set of Dial Gauges.

Figure 12. Rotating the Mechanical Jack.

E. Testing Program

The following section describes the experimental work performed through this study:

- The empty tank is placed in a horizontal position, vacuumed, and cleaned from any foreign materials. The required volume of sand, based on the considered relative density, was placed in four layers. The top level of each layer was marked on the inner surface of the container, and each layer was compacted by using a plate and a rammer, Figure (9).
- The proving ring and the horizontal loading bar were fixed in their positions, Figure (10). The horizontal loading bar was moved, until it touches the surface of the concrete sample which is rested on the soil surface.
- The sample cap is placed on the concrete sample in order to assure positioning of loads, then applying a normal load N on the top of the sample cover to apply a vertical normal stress. A horizontal dial gauge is set in its position as indicated in Figure (11).
- Setting up the test model takes about four hours, then loads were applied gradually and kept constant for about 4 hours, then test was performed.
- The load was applied to the footing sample through the mechanical screw jack, where the arm of the screw was rotated at constant loading rate of 0.12mm/min, as shown in Figure (12). The load was applied continuously until failure occurs, which is a great shear displacement with a constant load after increasing the load to its maximum value.

▪ EXPERIMENTAL RESULTS

This section presents all of the results for interface friction angles tests that were conducted in the laboratory using the modified direct shear test. Three different thicknesses of geomembranes including 3, 4 and 6 mm were used to investigate the effect of thickness on produced interface shear stress.

For all of specimens, Shear tests were conducted under a normal stress of 25, 50 and 100 kPa. The peak and residual shear stress were obtained right away after applying the normal stress on the sample. The interface friction angles for all tests are determined from the load and shear displacement relationships.

The samples were tested with a horizontal displacement approximately 12 mm [17]. In this study, all tests were performed under dry condition. Test's results showed that the peak interface shear resistance was typically developed at small shear displacements ranging between 1 to 2 mm or less [18], while the relatively stabilized residual interface shear resistance was developed at larger shear displacements. The peak and residual shear stress envelopes for both concrete and various geomembranes interfaces contacting with the sand are plotted in Figures (13) and (14). These envelopes can be described using Mohr-Coulomb criterion:

$$\tau = \sigma_n \tan(\delta) + C$$

Where:

τ = the peak or residual shear stress.

σ_n = the normal stress.

δ = the peak or residual angle of friction.

c = the peak or residual adhesion.

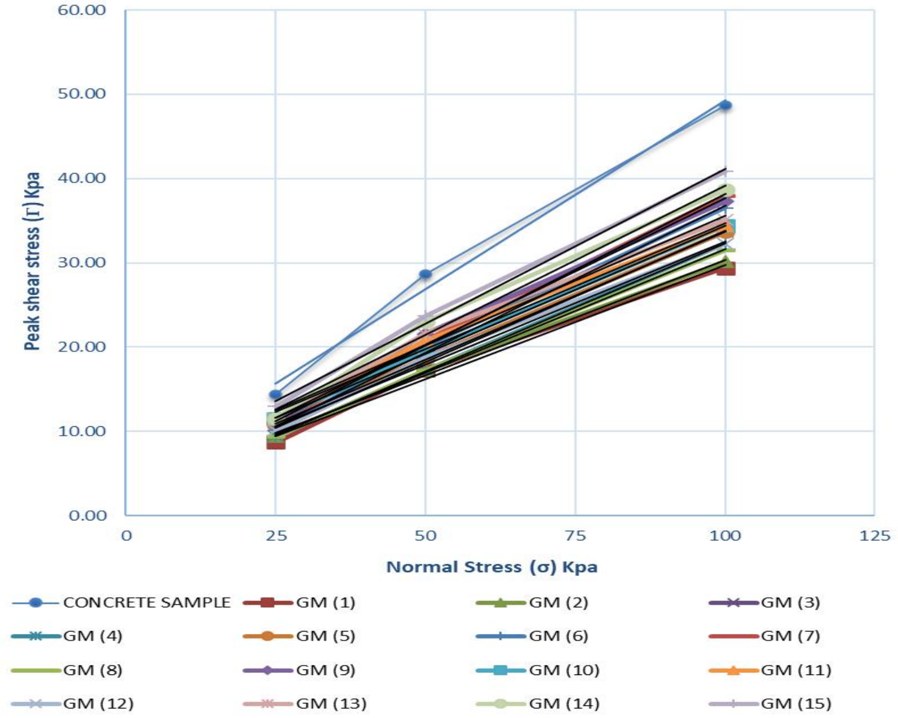

Figure 13. Normal stress and peak interface shear stress envelopes for both concrete and various geomembranes interfaces contacting with the sand.

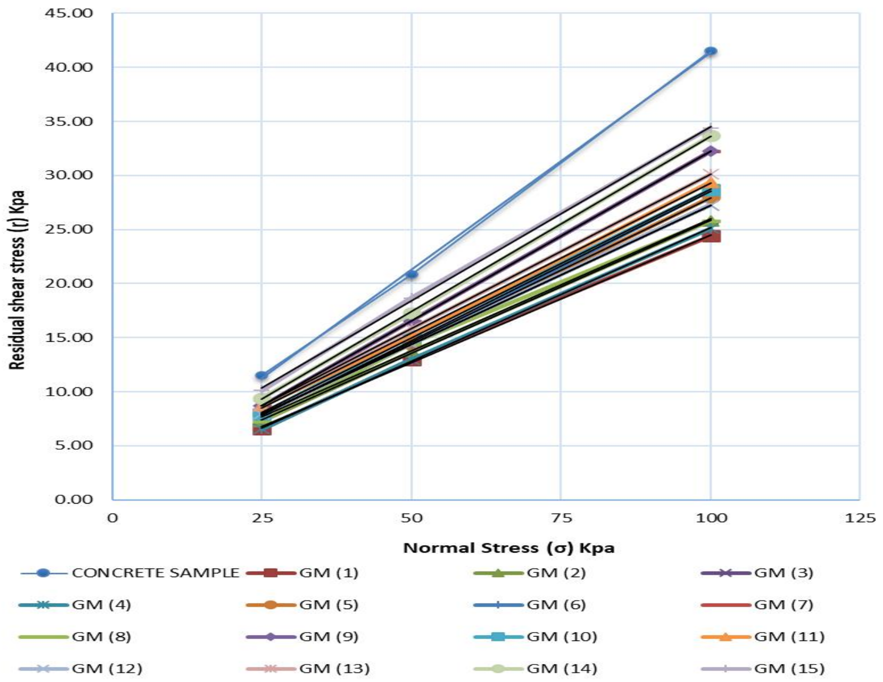

Figure 14. Normal stress and residual interface shear stress envelopes for both concrete and various geomembranes interfaces contacting with the sand.

IV. ANALYSIS AND DISCUSSION

In comparing results from this study, a non-dimensional factor E known as the efficiency ratio is used, which is expressed as the normalized values of the interface friction angles to that of the given soil.

$$E\phi = \frac{\mathrm{TAN}\ (\delta)}{\mathrm{TAN}\ (\phi)}$$

Where:
Eϕ = Efficiency ratio.
δ = peak or residual interface friction angles (degrees).
ϕ = angle of internal friction of the sand (degrees).

Table (3) shows a summary of the test results conducted on the un-protected concrete and the insulated concrete using different types of geomembranes with sand. Results of the normal stresses, peak shear stresses, peak angles of friction, efficiency ratio of peak friction angles (Eϕp), residual shear stresses, residual angles of friction, and efficiency ratio of residual friction angles (Eϕr) for each geomembranes types, are presented.

Figures (15) and (16) represent the efficiency ratios for developed peak friction angles and residual friction angles respectively for concrete and various types of geomembranes.

Table 3. Summary of interface shear stress results.

Interface	Normal Stress (KPa)	Peak Shear Stress (KPa)	Peak Friction angle, (δp°)	Efficiency Ratio of Peak Friction Angle, (Eϕp)	Residual Shear Stress (KPa)	Residual Friction Angle, (δr°)	Efficiency Ratio of Residual Friction Angle, (Eϕr)
concrete	25	14.41	24.17	0.67	11.55	21.89	0.6
	50	28.69			20.83		
	100	48.68			41.54		
GM (1)	25	8.69	15.18	0.40	6.55	13.31	0.35
	50	17.26			12.98		
	100	29.40			24.40		
GM (2)	25	9.41	15.29	0.41	7.27	13.86	0.37
	50	17.26			13.69		
	100	30.11			25.83		
GM (3)	25	10.12	17.33	0.46	7.98	14.41	0.38
	50	18.69			14.41		
	100	33.68			27.26		
GM (4)	25	9.41	16.91	0.45	6.55	13.86	0.37
	50	17.26			12.98		
	100	32.26			25.12		
GM (5)	25	10.84	16.91	0.45	7.98	14.96	0.40
	50	18.69			14.41		
	100	33.68			27.97		
GM (6)	25	10.12	19.23	0.52	7.98	15.50	0.41
	50	20.12			14.41		
	100	36.54			28.69		
GM (7)	25	10.84	19.75	0.53	8.69	17.44	0.47
	50	20.83			16.55		
	100	37.97			32.26		
GM (8)	25	9.41	16.37	0.44	7.27	13.76	0.36
	50	17.26			14.41		
	100	31.54			25.83		
GM (9)	25	10.84	19.13	0.51	8.69	17.44	0.47
	50	21.55			16.55		
	100	37.25			32.26		
GM (10)	25	11.55	16.91	0.45	7.98	15.40	0.41
	50	19.40			15.12		
	100	34.40			28.69		
GM (11)	25	11.55	16.69	0.44	8.69	15.50	0.41
	50	20.83			15.12		
	100	34.40			29.40		
GM (12)	25	10.12	16.26	0.43	7.98	14.41	0.38
	50	18.69			14.41		
	100	32.26			27.26		
GM (13)	25	11.55	17.12	0.46	8.69	15.94	0.42
	50	21.55			15.83		
	100	35.11			30.11		
GM (14)	25	11.55	19.54	0.53	9.41	17.97	0.48
	50	22.97			17.26		
	100	38.68			33.68		
GM (15)	25	12.98	20.16	0.54	10.12	17.86	0.48
	50	23.69			18.69		
	100	40.82			34.40		

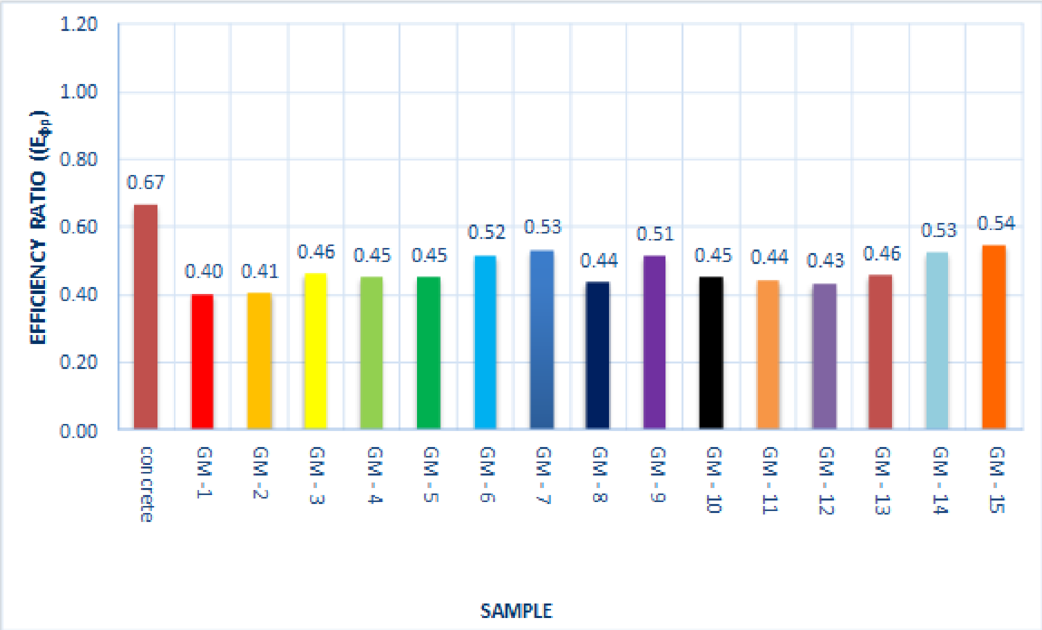

Figure 15. Efficiency ratio of peak friction angle (Eϕp).

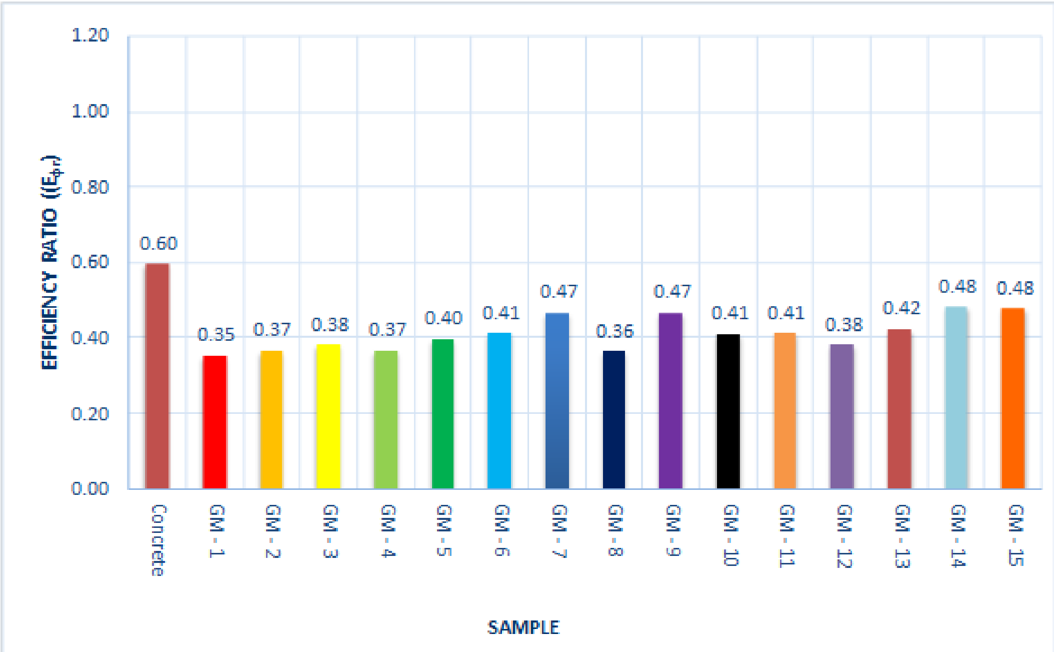

Figure 16. Efficiency ratio of peak residual friction angle (Eϕr).

The peak and residual friction angles between various types of insulation geomembranes and sand are significantly lower than the peak and residual friction angles between the un-protected concrete and sand. This is attributed to the fact that the use of insulation geomembranes adversely affects the developed peak and residual friction angles between the surface of buried concrete elements, as retaining walls, foundations, and the surrounding soils. The developed peak friction angles results for the un-protected concrete and different types of geomembranes are substantially less than the internal friction angle of the used sand soil (34.0°). The developed peak interface friction angle is measured to be of a value of (24.17°), for un-protected concrete-sand interface without geomembranes. The peak interface friction angle of the un-protected concrete-sand interface (without geomembranes) is measured to be higher than the mobilized peak friction angle of the geomembranes-sand interface, under the same tests conditions, by a value ranging between (4.01° - 8.99°). It is clearly noticed that the peak friction angles of the Slated geomembranes are higher than the peak friction angles of the smooth geomembranes. The developed residual friction angles results for the un-protected concrete and different types of geomembranes are substantially less than the internal friction angle of the used sand soil (34.0°). The developed residual interface friction angle is measured to be of a value of (21.89°), for un-protected concrete-sand interface without geomembranes. The residual interface friction angle of the un-protected concrete-sand interface (without geomembranes) is measured to be higher than the mobilized residual friction angle of the geomembranes-sand interface, under the same tests conditions by a value ranging between (3.92° - 8.58°). It is clearly noticed that the residual friction angles of the Slated geomembranes are higher than the residual friction angles of the smooth geomembranes.

In comparing results of sand and geomembranes interface with results of sand and concrete interface to quantify the reduction in the shear resistance of soils in contact with buried concrete elements protected due to using different types of geomembranes, a non-dimensional reduction factor of the peak and residual interface friction angles (E) known as the reduction factor is used [19]. This reduction factor is expressed as:

$$E = \frac{\mathrm{TAN}\ (\delta g)}{\mathrm{TAN}\ (\delta c)}$$

Where:

Ec = the reduction factor.

δg = peak or residual interface friction angle between sand and geomembranes (degrees).

δc = peak friction angle between concrete and soil (degrees).

Figures (17) and (18) represent the reduction factor for peak and residual interface friction angles respectively for concrete and various types of geomembranes.

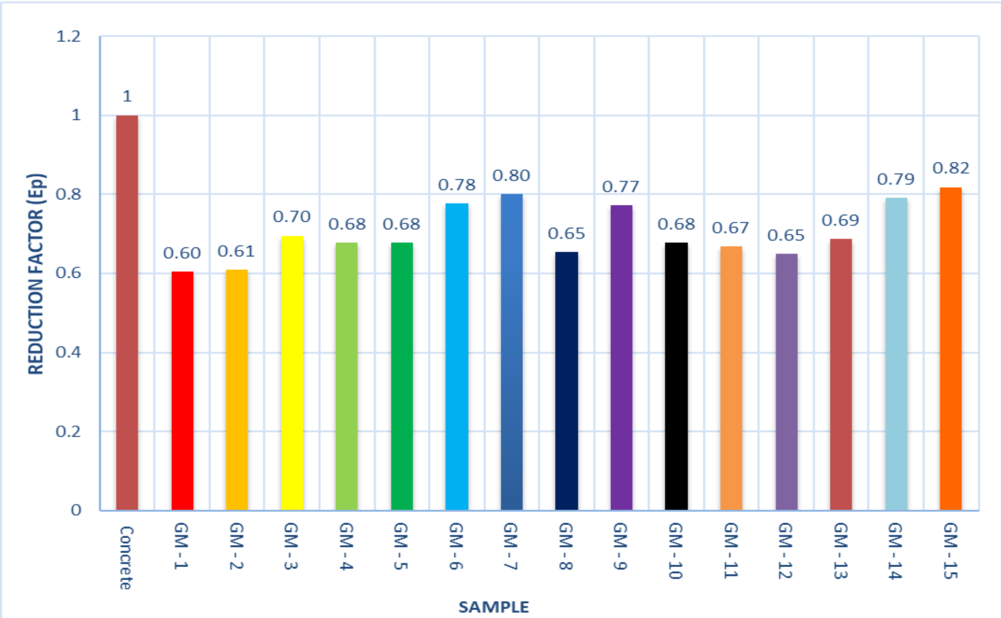

Figure 17. Reduction factor of peak interface friction angles (EP).

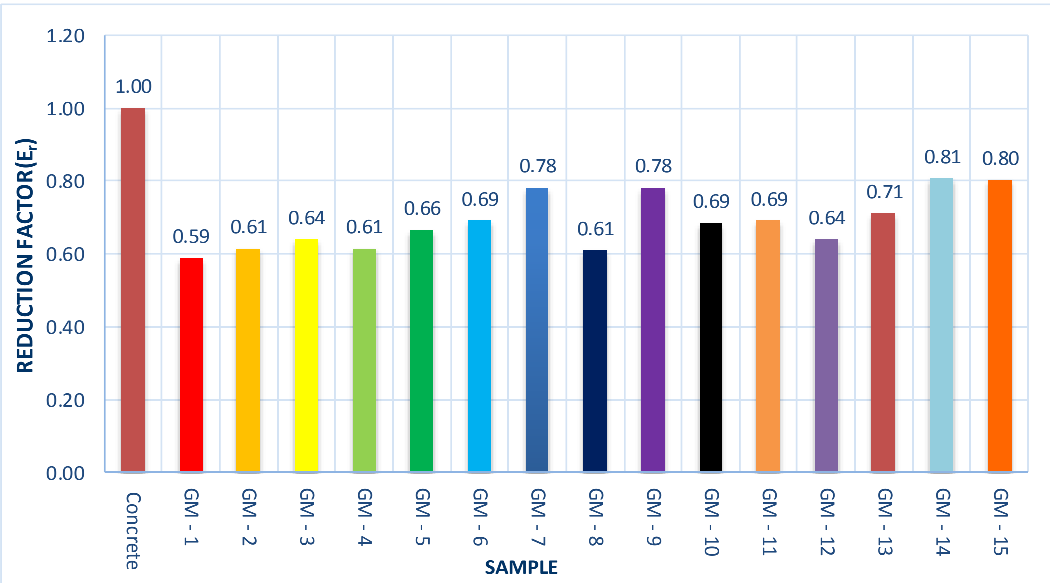

Figure 18. Reduction factor of peak interface friction angles (Er).

Table 4. Summary of interface shear stress results.

Interface	Normal Stresses (KPa)	Peak Shear Stresses (KPa)	Peak Friction Angle, (δp°)	Reduction factor, (Ep)	Residual Shear Stresses (KPa)	Residual Friction Angle, (δr°)	Reduction factor, (Er)
GM (1)	25	8.69	15.18	0.60	6.55	13.31	0.59
	50	17.26			12.98		
	100	29.40			24.40		
GM (2)	25	9.41	15.29	0.61	7.27	13.86	0.61
	50	17.26			13.69		
	100	30.11			25.83		
GM (3)	25	10.12	17.33	0.70	7.98	14.41	0.64
	50	18.69			14.41		
	100	33.68			27.26		
GM (4)	25	9.41	16.91	0.68	6.55	13.86	0.61
	50	17.26			12.98		
	100	32.26			25.12		
GM (5)	25	10.84	16.91	0.68	7.98	14.96	0.67
	50	18.69			14.41		
	100	33.68			27.97		
GM (6)	25	10.12	19.23	0.78	7.98	15.50	0.69
	50	20.12			14.41		
	100	36.54			28.69		
GM (7)	25	10.84	19.75	0.80	8.69	17.44	0.78
	50	20.83			16.55		
	100	37.97			32.26		
GM (8)	25	9.41	16.37	0.65	7.27	13.76	0.61
	50	17.26			14.41		
	100	31.54			25.83		
GM (9)	25	10.84	19.13	0.77	8.69	17.44	0.78
	50	21.55			16.55		
	100	37.25			32.26		
GM (10)	25	11.55	16.91	0.68	7.98	15.40	0.69
	50	19.40			15.12		
	100	34.40			28.69		
GM (11)	25	11.55	16.69	0.67	8.69	15.50	0.69
	50	20.83			15.12		
	100	34.40			29.40		
GM (12)	25	10.12	16.26	0.65	7.98	14.41	0.64
	50	18.69			14.41		
	100	32.26			27.26		
GM (13)	25	11.55	17.12	0.69	8.69	15.94	0.71
	50	21.55			15.83		
	100	35.11			30.11		
GM (14)	25	11.55	19.54	0.79	9.41	17.97	0.81
	50	22.97			17.26		
	100	38.68			33.68		
GM (15)	25	12.98	20.16	0.82	10.12	17.86	0.80
	50	23.69			18.69		
	100	40.82			34.40		

Table 4 illustrates the reduction factor of the peak and residual interface friction angles for various types of geomembranes, in the form of the normal stresses and their corresponding peak shear stresses, peak interface friction angles, reduction factor of peak interface friction angles, residual shear stresses, residual interface friction angles and reduction factor of residual interface friction angles. It is also found that the peak and residual interface friction angles between the sand and the geomembranes interfaces ranged from 59 % to 82 % of the peak and residual interface friction angles between the sand and concrete interface.

V. CONCLUSIONS

This paper describes a study on sand and geomembranes interfaces frictional behavior by using a series of tests were performed in the laboratory by using a modified direct shear tests to determine the interface friction angles between the sand and the geomembranes. The study shows that the interface sliding between the sand and the geomembranes, peak and residual strength values are mobilized during the testing. It must be noted that the results provided by the analysis are based upon the findings of this investigation and are limited to the materials and the considered boundary conditions during the study. The experimental tests, developed and discussed throughout this research work stages, has given the possibility to draw out some conclusion, which are summarized in the following sections;

- This study can be applied for sandy soil under stress limit up to 100 KPA.
- The peak interface shear resistance develops at a small shear displacement ranging between 1 to 2 mm, or less, while the residual interface shear resistance develops at larger shear displacements.
- The shear resistance-associated with the slated surface insulation geomembranes are greater than the shear resistance associated with the smooth surface insulation geomembranes.

- The developed residual and peak interface friction angles between the sand and the insulation geomembranes ranges from 59 % to 82 % of the corresponding peak and residual interface friction angles between sand and un-protected concrete.
- The developed residual and peak interface friction angles between sand and geomembranes range from 40% to 54% and from 35% to 48% of the internal friction angle of sand respectively.
- The developed residual and peak interface friction angles between sand and un-protected concrete interfaces is 67% and 60% of the internal friction angle of sand respectively.
- The developed residual and peak interface friction angles (δp and δr), between the sand and the insulation geomembranes vary from 15.18° to 20.16° and from 13.31° to 17.97° respectively.
- These conclusions are limited to the considered materials and the boundary conditions.

Funding: This research has not received any type of funding.

Conflicts of Interest: The authors declare that there is no conflict of interest.

REFERENCES

[1] M. A. Jahanfar, “Landfill slope stability risk assessment.” 2014.
[2] J. P. Martin, R. M. Koerner, and J. E. Whitty, “Experimental friction evaluation of slippage between geomembranes, geotextiles and soils,” in Proceedings of the International Conference on Geomembranes, 1984, vol. 1, pp. 191–196.
[3] M. Jogi, “A method for measuring smooth geomembrane/soil interface shear behaviour under unsaturated conditions.” 2005.
[4] C. ASTM, “Standard test method for compressive strength of hydraulic cement mortars (using 2-in. or [50-mm] cube specimens),” Annu. B. ASTM Stand., vol. 4, 2016.
[5] J. P. Giroud, J. Darrasse, and R. C. Bachus, “Hyperbolic expression for soil-geosynthetic or geosynthetic-geosynthetic interface shear strength,” Geotext. Geomembranes, vol. 12, no. 3, pp. 275–286, 1993.
[6] M. E. Smith and K. Criley, “Interface shear strength is not for the uninitiated,” Geotech. Fabr. Rep., vol. 13, p. 28, 1995.
[7] D. Negussey, W. K. D. Wijewickreme, and Y. P. Vaid, “Geomembrane interface friction,” Can. Geotech. J., vol. 26, no. 1, pp. 165–169, 1989.
[8] R. Effendi, “Interface Friction of Smooth Geomembranes and Ottawa Sand,” INFO-TEKNIK, vol. 12, no. 1, pp. 61–72, 2016.
[9] V. K. Veerla and K. Srinivas, “A study on soil interface interaction,” Mater. Today Proc., vol. 51, pp. 2561–2568, 2022.
[10] D. Adeleke, D. Kalumba, L. Nolutshungu, J. Oriokot, and A. Martinez, “The Influence of Asperities and Surface Roughness on Geomembrane/Geotextile Interface Friction Angle,” Int. J. Geosynth. Gr. Eng., vol. 7, no. 2, pp. 1–12, 2021.
[11] S. Kazempoor and A. N. A. R. Mahboubi, “Surcharge Stress Infulence On Smooth Geomembrane–Soil Interface Shear Behavior”.
[12] R. Ziaie Moayed, M. Alibolandi, and A. Alizadeh, “Specimen size effects on direct shear test of silty sands,” Int. J. Geotech. Eng., vol. 11, no. 2, pp. 198–205, 2017.
[13] K. Zahran and H. El Naggar, “Effect of sample size on TDA shear strength parameters in direct shear tests,” Transp. Res. Rec., vol. 2674, no. 9, pp. 1110–1119, 2020.
[14] K. L. Fishman and S. Pal, “Further study of geomembrane/cohesive soil interface shear behavior,” Geotext. Geomembranes, vol. 13, no. 9, pp. 571–590, 1994.
[15] H. T. Eid and C. K. Doerfler, “Effect of shear displacement rate on internal shear strength of a reinforced geosynthetic clay liner,” Geosynth. Int., vol. 6, no. 3, pp. 219–239, 1999.
[16] E. J. Triplett and P. J. Fox, “Shear strength of HDPE geomembrane/geosynthetic clay liner interfaces,” J. Geotech. Geoenvironmental Eng., vol. 127, no. 6, pp. 543–552, 2001.
[17] R. B. Gilbert and R. J. Byrne, “Strain-softening behavior of waste containment system interfaces,” Geosynth. Int., vol. 3, no. 2, pp. 181–203, 1996.
[18] D. R. V Jones and N. Dixon, “Shear strength properties of geomembrane/geotextile interfaces,” Geotext. Geomembranes, vol. 16, no. 1, pp. 45–71, 1998.
[19] C. Hsieh and M.-W. Hsieh, “Load plate rigidity and scale effects on the frictional behavior of sand/geomembrane interfaces,” Geotext. Geomembranes, vol. 21, no. 1, pp. 25–47, 2003.